JOURNAL OF VIROLOGY, Sept. 2007, p. 9426–9436 Vol. 81, No. 17
0022-538X/07/$08.00+0 doi:10.1128/JVI.00747-07


# An RNA Pseudoknot in the 3′ End of the Arterivirus Genome Has a Critical Role in Regulating Viral RNA Synthesis▽

Nancy Beerens and Eric J. Snijder*

*Molecular Virology Laboratory, Department of Medical Microbiology, Center of Infectious Diseases, Leiden University Medical Center, PO Box 9600, 2300 RC Leiden, The Netherlands*

Received 5 April 2007/Accepted 13 June 2007

**In the life cycle of plus-strand RNA viruses, the genome initially serves as the template for both translation of the viral replicase gene and synthesis of minus-strand RNA and is ultimately packaged into progeny virions. These various processes must be properly balanced to ensure efficient viral proliferation. To achieve this, higher-order RNA structures near the termini of a variety of RNA virus genomes are thought to play a key role in regulating the specificity and efficiency of viral RNA synthesis. In this study, we have analyzed the signals for minus-strand RNA synthesis in the prototype of the arterivirus family, equine arteritis virus (EAV). Using site-directed mutagenesis and an EAV reverse genetics system, we have demonstrated that a stem-loop structure near the 3′ terminus of the EAV genome is required for RNA synthesis. We have also obtained evidence for an essential pseudoknot interaction between the loop region of this stem-loop structure and an upstream hairpin residing in the gene encoding the nucleocapsid protein. We propose that the formation of this pseudoknot interaction may constitute a molecular switch that could regulate the specificity or timing of viral RNA synthesis. This hypothesis is supported by the fact that phylogenetic analysis predicted the formation of similar pseudoknot interactions near the 3′ end of all known arterivirus genomes, suggesting that this interaction has been conserved in evolution.**

Following genome translation and replication complex formation, the RNA synthesis of plus-strand RNA viruses starts with the production of a full-length minus-strand copy of the genomic RNA, which will serve as template for replication. To maintain the integrity of the genome, the initiation of minus-strand RNA synthesis has to occur at or close to the 3′ terminus of the RNA molecule. Consequently, prior to the initiation of minus-strand RNA synthesis, the replicase complex must be specifically targeted to recognition signals in the viral genome. Plus-strand RNA virus genomes are involved in a variety of processes and interactions including translation, replication, transcription, and encapsidation. The balance between these processes must be properly maintained to ensure efficient viral proliferation.

Over the past decade, it has been increasingly recognized that RNA-mediated processes can be controlled by conformational switches that are based on alternative RNA structures (20, 27, 42). Recent evidence, obtained using several unrelated viruses, suggests that such conformational switches may be needed to hide and expose specific RNA signals in the 3′ end of viral genomes. Some viruses appear to activate these switches by changing the conformation of 3′ proximal structures (16, 28, 33, 51). For example, barley yellow dwarf virus is proposed to repress minus-strand RNA synthesis by embedding its genomic 3′ end in a "pocket" structure, thereby making it unavailable to the RNA-dependent RNA polymerase (RdRp) complex (16). A similar molecular switch was proposed for several coronavirus genomes, involving sequences within stem-loop and RNA pseudoknot structures in the 3′ untranslated region (UTR) (9, 12, 13, 47). In addition, cellular factors or viral proteins may affect the balance between such alternative structural conformations (28, 38). For example, the 3′ terminus of the alfalfa mosaic virus genome can adopt an alternative conformation by the formation of a pseudoknot. Binding of the viral coat protein to the genomic 3′ end inhibits minus-strand RNA synthesis by interfering with the formation of this pseudoknot (28). These findings among different groups of RNA viruses suggest that RNA conformational switches may control the exposure of RNA signals recognized by the RdRp complex to regulate both the timing and the levels of viral RNA synthesis.

The plus-strand RNA genomes of members of the order *Nidovirales* (arterivirus, coronavirus, torovirus, and ronivirus; for reviews, see references 11 and 39) are capped at their 5′ end and polyadenylated at their 3′ end. Nidovirus replication occurs in the cytoplasm of the infected cell and is driven by a complex of 13 to 16 replicase subunits, including the viral RdRp complex. In addition to producing full-length plus- and minus-strand molecules, the RNA-synthesizing machinery of nidoviruses engages in the production of a nested set of 3′ coterminal subgenomic (sg) mRNAs. In the case of corona- and arteriviruses, these transcripts also contain a common 5′ leader sequence that is derived from the genomic 5′ end. Subgenomic RNA production relies on a unique mechanism of discontinuous RNA synthesis that is thought to operate during minus-strand RNA synthesis and serves to produce the subgenome-length minus-strand templates for mRNA synthesis (for reviews see references 30, 35, and 36 and references therein). Thus, for nidoviruses, both genome replication and sg RNA synthesis are thought to initiate at the 3′ end of the viral genome RNA.

Equine arteritis virus (EAV) is the prototype virus of the arterivirus family. In a previous study, we investigated the RNA secondary structure of the 3′ end of the 12.7-kb EAV

* Corresponding author. Mailing address: Molecular Virology Laboratory, Department of Medical Microbiology, Leiden University Medical Center, LUMC P4-26, PO Box 9600, 2300 RC Leiden, The Netherlands. Phone: 31 71 5261657. Fax: 31 71 5266761. E-mail: e.j.snijder@lumc.nl.

▽ Published ahead of print on 20 June 2007.

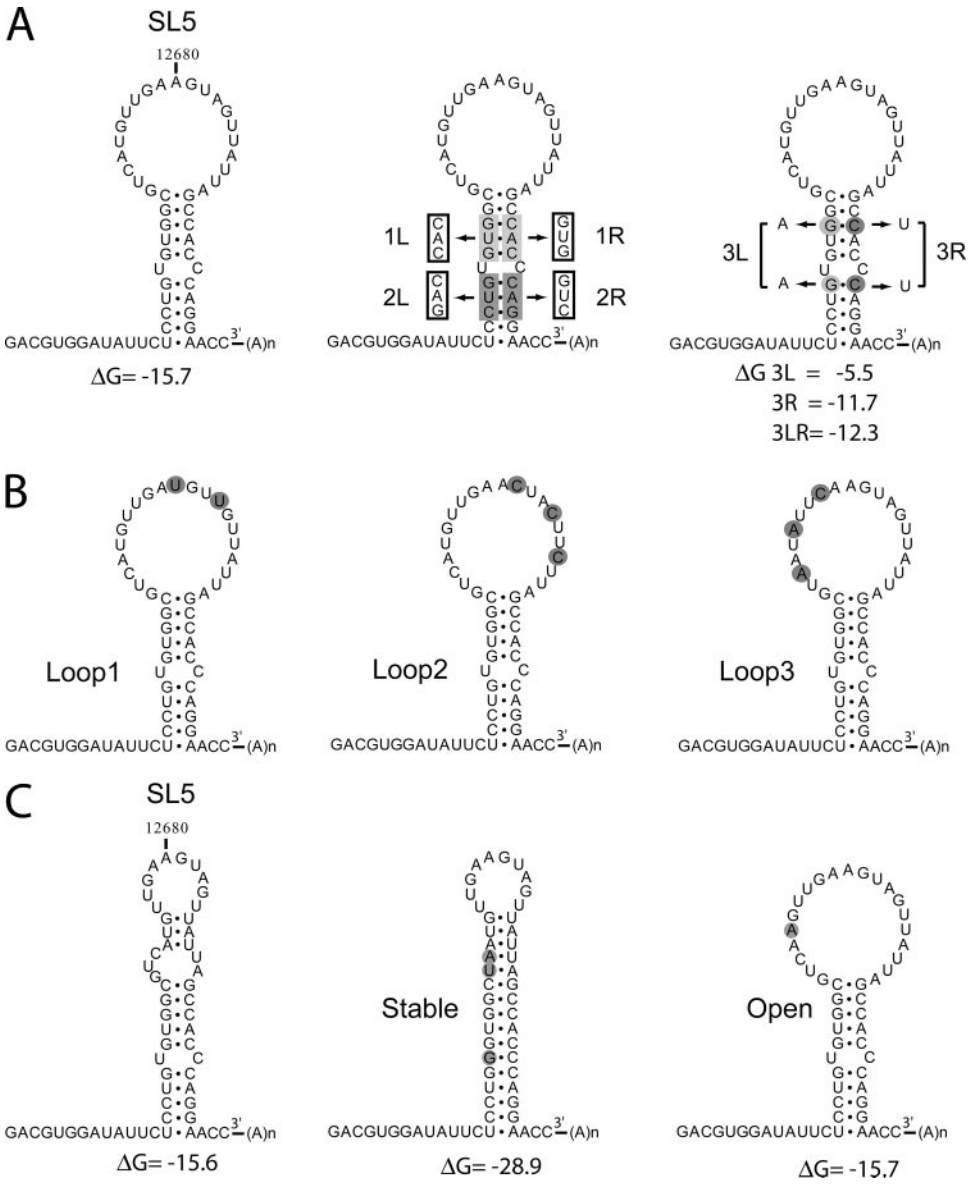


FIG. 1. RNA secondary structure models for the 3′ UTR of wild-type EAV and SL5 mutants. (A) Mutations were introduced in the SL5 stem region. Mutant 1L has a 3-nucleotide substitution on the left side of the stem, and mutant 1R on the right side. Mutations 1L and 1R are complementary, and base pairing is restored in the double mutant 1LR. Similar mutations were also introduced in the lower stem segment (2L, 2R, and 2LR). The stability of the stem region was targeted in mutants 3L, 3R, and 3LR by the replacement of two G-C base pairs. (B) Mutants Loop1, Loop2, and Loop3 contain point mutations in the SL5 loop region. (C) Mfold prediction of an alternative structure for the SL5 stem-loop with similar stability, in which part of the loop region is closed by base pairing. This alternative structure was stabilized by the mutations introduced in mutant Stable and prevented by the mutation introduced in mutant Open.

genome (3). Two stem-loop structures were implicated in the initiation of viral RNA synthesis SL5 (Fig. 1A), located in the 3′ UTR, and SL4, located in the most 3′ proximal gene of the EAV genome, which encodes the nucleocapsid (N) protein. To gain insight into the mechanisms involved in the regulation of EAV minus-strand RNA synthesis, we have now further characterized the RNA signals near the 3′ end of the genome. We demonstrate that the structure of the SL5 stem is important for RNA synthesis, as is its large single-strand loop region. We have also obtained evidence for a pseudoknot interaction between the loop region of SL5 and the SL4 hairpin, a structural feature that was found to be essential for viral RNA synthesis. We propose that the formation of this pseudoknot interaction may constitute a molecular switch that could regulate the specificity or timing of viral RNA synthesis. This notion was supported by a phylogenetic analysis revealing that the 3′ proximal pseudoknot interaction has likely been conserved in arterivirus evolution.

## MATERIALS AND METHODS

**Site-directed mutagenesis and EAV reverse genetics.** Mutations in the 3′ proximal domain of the EAV genome were engineered in shuttle plasmids by

standard site-directed PCR mutagenesis. After sequence analysis, restriction fragments containing the desired mutations were transferred to full-length clone pEAV211 (43). Full-length transcripts were generated in vitro from XhoI-linearized plasmid DNA using T7 RNA polymerase (Invitrogen). In vitro transcription was performed in the presence of a cap analog (New England Biolabs), and the reaction conditions have been described previously (45). Following DNase I treatment and phenol extraction, unincorporated free nucleotides were removed using an RNase-free MicroBioSpin P-30 column (Bio-Rad). Subsequently, RNA was isopropanol precipitated and dissolved in water. RNA concentration was measured by UV spectroscopy, and the integrity of the RNA transcripts was verified by agarose gel electrophoresis.

**Cells and transfections.** Baby hamster kidney cells (BHK-21; ATCC CCL10) were used for EAV full-length RNA transfection experiments as described previously (45). Cells were grown to subconfluence, trypsinized, washed with phosphate-buffered saline (PBS), and resuspended in PBS at a concentration of $5 \times 10^7$ cells per ml. Equal amounts (6 μg) of full-length EAV RNA were used to transfect 100 μl of the BHK-21 cell suspension ($5 \times 10^6$ cells) by electroporation using a Nucleofector (Amaxa) system according to the supplier's protocol (kit T, program T-20). After transfection, the cells were seeded and incubated at 39.5°C.

**Analysis of virus replication.** Immunofluorescence dual-labeling assays with a rabbit antiserum specific for EAV nsp3 and mouse monoclonal antibody 3E2 directed against the EAV N protein were performed as described previously (44) at different time points after transfection. For intracellular RNA isolation, cells were lysed at 14 h posttransfection, and RNA was isolated using the acidic phenol method, as described previously (29). Viral RNA was analyzed with denaturing formaldehyde-agarose gels and hybridized with the radioactively labeled oligonucleotide probe E868 (antisense, genome positions 12270 to 12289) which recognizes both genomic and subgenomic plus-strand RNAs. Dried gels were imaged using phosphorimager screens, which were scanned with a Personal Molecular Imager FX (Bio-Rad) after exposure. Virus titration using plaque assays was done as described previously (23). BHK-21 cells were grown to subconfluence and infected with a serial dilution of the sample to be tested. Infection was performed for 1 h at 39.5°C, after which an overlay of 1% agarose in medium was applied. Plaques were detected after incubation at 39.5°C for 2 to 3 days.

**Analysis of revertants.** The 3′ proximal region of the EAV genome was amplified from intracellular RNA (see description above), using reverse transcription (RT)-PCR. For the RT reaction, an 18-nucleotide oligo(dT) primer was used to prime reverse transcription from the poly(A) tail. In the subsequent PCR, the reverse primer oligo(dT) and the forward primer E817 (positions 12288 to 12308) were used. The RT-PCR product was used for direct population sequencing or was cloned into a plasmid using a TOPO TA cloning kit (Invitrogen), after which individual clones were sequenced. To analyze the impact of the acquired mutations on the viral phenotype, sequences derived from the revertants were cloned back into full-length clone pEAV211. Introduction of the revertant sequences was verified by sequence analysis, and full-length clones were used to launch (potential) revertant viruses as described above.

**Phylogenetic analysis.** The sequences of different arteriviruses (EAV, porcine reproductive and respiratory syndrome virus [PRRSV], simian hemorrhagic fever virus [SHFV], and lactate dehydrogenase-elevating virus [LDV]) were retrieved and aligned using the nucleotide-nucleotide BLAST service at NCBI. RNA secondary structures were predicted using the Zuker algorithm (52) on the Mfold Web server (53). RNA secondary structure drawings were created using RNAviz software (6).

## RESULTS

**Design of SL5 mutants.** To study the role of the 3′ proximal SL5 hairpin structure (Fig. 1A) (3) in viral RNA synthesis, mutations were introduced in an EAV full-length cDNA clone (45) that served as the basis for reverse genetics experiments. To study the importance of the SL5 stem, the upper stem segment (segment 1) was mutated by a 3-nucleotide substitution, either on its left side (mutant 1L) or on the right side (mutation 1R) as shown in Fig. 1A. Mutations 1L and 1R were complementary, and base pairing should be restored in double mutant 1LR containing both sets of mutations. Similar mutations were introduced in the lower-stem segment (segment 2; mutants 2L, 2R, and 2LR). In addition, the importance of the stability of the stem region was probed by the substitution of two G-C base pairs, one in each stem segment (Fig. 1A). In mutant 3L, these base pairs were replaced by A-C mismatches, in mutant 3R by G-U base pairs, and in mutant 2LR by A-U base pairs.

TABLE 1. Viability of SL5 stem mutants[a]

| Mutant | IFA at the indicated time points posttransfection | | | Titer (PFU/ml) at 24 h posttransfection |
|---|---|---|---|---|
| | 14 h | 24 h | 40 h | |
| wt | ++ | +++ | X | $9 \times 10^6$ |
| 1L | − | − | − | ND |
| 1R | − | − | − | ND |
| 1LR | ++ | +++ | X | $5 \times 10^6$ |
| 2L | − | − | − | ND |
| 2R | − | − | − | ND |
| 2LR | ++ | +++ | X | $3 \times 10^6$ |
| 3L | − | − | − | ND |
| 3R | − | − | − | ND |
| 3LR | + | ++ | +++ | $2 \times 10^4$ |

[a] X, cells were detached and dying from infection. ND, not determined.

The SL5 hairpin contains a large single-stranded loop region, as was previously predicted by Mfold RNA secondary structure analysis (52, 53) and verified with biochemical probing experiments (3). To study the importance of this loop region in RNA synthesis, mutants Loop1, Loop2, and Loop3 were generated which contained various point mutations in the loop region (Fig. 1B). In addition, the Mfold program predicted an alternative SL5 structure with similar stability, in which part of the loop sequence is engaged in base pairing (Fig. 1C). To study the possible contribution of this alternative structure to RNA synthesis, two mutants were generated (Fig. 1C). In mutant Stable, substitutions were introduced on the left side of the stem, which were complementary to bulge nucleotides on the right side of the stem. This resulted in a modified SL5 structure with an extended, more stable stem region and part of the loop sequence engaged in base-pairing interactions. In mutant Open, on the other hand, the formation of this putative alternative structure was prevented by a single point mutation.

**The SL5 structure and loop region are critical for EAV RNA synthesis.** BHK-21 cells were transfected with infectious RNA transcribed in vitro from wild-type and mutant EAV full-length cDNA clones. For an initial rapid screening, the production of viral proteins in transfected cells was monitored by dual-labeling immunofluorescence assays (IFA) using antisera recognizing nonstructural protein 3 and the structural N protein, which served as indicators for genome replication and sg mRNA synthesis, respectively (summarized in Table 1). In addition, supernatants harvested from the transfected cell cultures were tested for the presence of progeny virus by using plaque assays (Table 1). No IFA signal or infectious progeny was detected for the mutants in which one side of the stem was mutated (1L, 1R, 2L, and 2R), whereas virus replication was comparable to that of the wild-type control in the case of double mutants 1LR and 2LR, in which the base-pairing possibilities to form the SL5 stem had been restored. The stability of the stem region also appeared important for virus viability. Replacing two G-C base pairs with A-U base pairs in mutant 3LR resulted in reduced IFA signals, a small-plaque phenotype, and a 450-fold

TABLE 2. Viability of SL5 loop mutants[a]

| Mutant | IFA at the indicated time points posttransfection | | | Titer (PFU/ml) at 24 h posttransfection |
|---|---|---|---|---|
| | 14 h | 24 h | 40 h | |
| wt | ++ | +++ | X | $2 \times 10^7$ |
| Loop1 | + | ++ | +++ | $5 \times 10^5$ |
| Loop2 | − | − | − | ND |
| Loop3 | − | − | − | ND |
| Open | ++ | +++ | X | $5 \times 10^6$ |
| Stable | − | − | − | ND |

[a] X, cells were detached and dying from infection. ND, not determined.

reduction of virus titer. Substitution with G-U base pairs in mutant 3R and disruption of base pairing in mutant 3L completely blocked virus replication. The viability of mutant Loop1 was reduced as illustrated by a smaller-plaque phenotype and 40-fold reduction in virus titer, whereas the Loop2 and Loop3 mutations completely abolished replication (Table 2). Mutant Open replicated efficiently, but no IFA signal or infectious progeny could be detected for mutant Stable (Table 2).

Synthesis of viral RNA (genomic and subgenomic) was analyzed after approximately one cycle of virus replication. For the wild-type virus, both the full-length genome (RNA1) as well as the sg mRNAs 2 to 7 were detected (Fig. 2). No RNA was produced for the single mutants 1L, 1R, 2L, and 2R, whereas all RNAs were produced at levels similar to those of the wild-type control by the double mutants 1LR and 2LR. No RNA synthesis was observed for mutants 3L and 3R, whereas all RNAs were produced by mutant 3LR, albeit at severely reduced levels. In this crippled mutant, genome replication and sg RNA synthesis were affected to the same extent.

All mutations introduced in the SL5 loop region were found to inhibit or block viral RNA synthesis (Fig. 2). Mutant Loop1 produced reduced levels of all RNAs, whereas no RNA signal was detected for mutants Loop2 and Loop3. RNA synthesis by mutant Open was just slightly reduced compared to that of the wild-type virus, and no RNA synthesis was observed for mutant Stable. The fact that mutant Open produced RNA at levels close to that of the wild type suggested that the alternative structure predicted for SL5 (Fig. 2B) does not play an important role in RNA synthesis. These results demonstrate that the structure and stability of the SL5 stem are important for RNA synthesis. In addition, sequences in the SL5 loop region were found to play a key role in viral RNA synthesis, presumably during the initiation of viral minus-strand RNA synthesis.

**Reversion of two SL5 mutants.** Upon prolonged culture of viruses with impaired replication properties, revertants with increased fitness can arise. Analysis of the changes in the genomes of such revertants may identify important RNA sequences and/or structures. At 72 h posttransfection, the first positive IFA signal was observed for cells transfected with mutants Stable and Loop2. To analyze the genetic changes in these revertants, RNA was isolated from infected cells, and the 3′ proximal domain of the EAV genome was amplified by RT-PCR. Population-based sequencing of the PCR product for the revertants of the Stable mutant produced an inconclusive result, probably due to the presence of a mixture of sequences. Therefore, this PCR product was cloned in a plasmid, and seven individual clones were analyzed (Fig. 3). Two of these clones contained an insertion in the upper part of the SL5 stem, and in addition, the G introduced into the lower part of the stem had reverted back to the wild-type U residue (St-rev1). One clone (St-rev2) contained the insertion lacking the 5′ G residue, and in four other clones, an additional G was lacking from the insertion (St-rev3), resulting in a sequence that differed at only one position (the U-to-A change) from that of the wild-type sequence (Fig. 3). After one additional virus passage, all of the eight clones analyzed were of the St-rev3 type, suggesting that reversion most likely started with an insertion that was further modified to gain replication capacity. Clones St-rev1 and St-rev2 may represent intermediates from an evolutionary pathway leading to the St-rev3 sequence, which differs from the wild-type sequence at only one position in the SL5 loop.

The population sequence of the Loop2 revertant revealed a

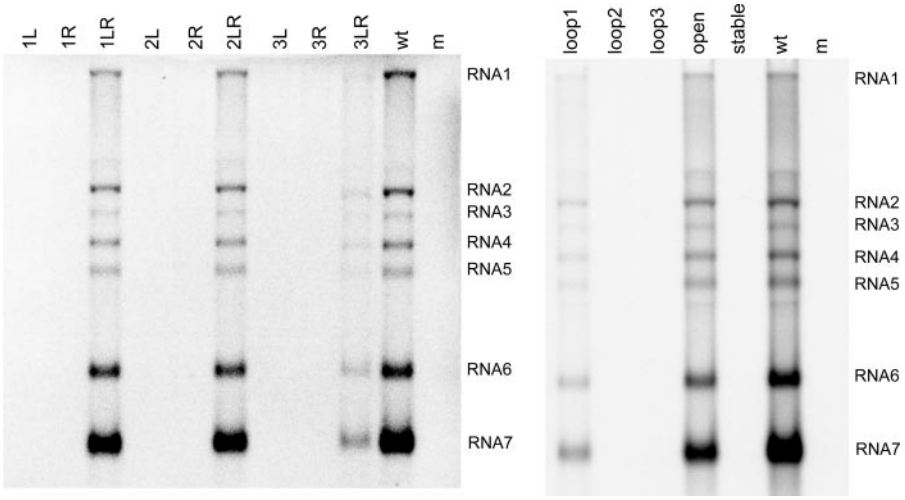


FIG. 2. RNA synthesis by wild-type EAV and SL5 mutants. Infectious RNA was transfected into BHK-21 cells, and intracellular RNA was isolated at 14 h posttransfection. The RNA was separated in a denaturing agarose gel and analyzed by hybridization to an oligonucleotide detecting all plus-stranded viral RNAs. The positions of the genome (RNA1) and sg mRNAs (RNA2 to RNA7) are indicated.

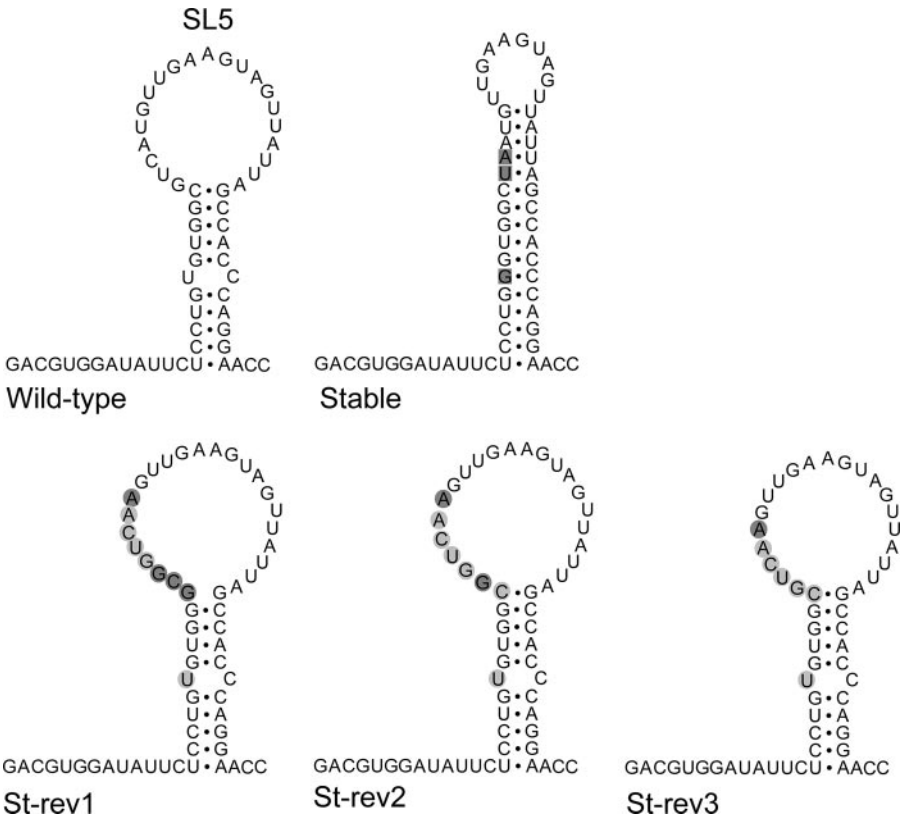


FIG. 3. Reversion of mutant Stable. The mutations originally introduced into mutant Stable are boxed. Upon sequence analysis, we identified two clones named St-rev1 that contained an insertion partly restoring the wild-type sequence and opening the loop region (insertions are shown in balls, wild-type residues are marked in light gray, mutant residues in dark gray). The sequence St-rev2 was obtained from one clone, the sequence St-rev3 from four clones. After one additional virus passage, all eight clones sequenced were of the St-rev3 type.

single second-site reversion directly upstream of the introduced mutations (Fig. 4A, L-rev1). In addition, sequencing of nine cloned PCR products was performed (Fig. 4A). Seven of these clones contained only the same reversion mutation identified by population sequencing (L-rev1). However, two clones had mutations in the SL4 region, suggesting an interaction between this domain and the SL5 region in which the Loop2 mutations had been introduced. Upon detailed analysis of the sequences, a potential SL4-SL5 base-pairing interaction was identified consisting of 10 base pairs interrupted by two mismatches (Fig. 4A and Fig. 5). One of the three mutations introduced in mutant Loop2 would result in the loss of one base pair in this duplex. The acquired mutation in L-rev1 would create an alternative base pair, filling one of the gaps in the original base paired region, and would thus strengthen the interaction. One clone (L-rev2) contained both the L-rev1 mutation and a mutation in SL4 that would create an additional base pair. Clone L-rev3 contained the original, mutated SL5 domain from mutant Loop2 but contained an SL4 mutation generating a novel base pair at the same position pinpointed by the L-rev1 revertant (Fig. 4A). To confirm that the acquired mutations were indeed the basis for reversion of the Loop2 mutant, they were introduced into the Loop2 mutant full-length cDNA clone, which originally was negative for virus replication (Table 2). Following transfection, virus replication was again monitored by IFA and plaque assays (Fig. 4A), and intracellular RNA synthesis was analyzed (Fig. 4B). Although the virus containing the L-rev2 sequence was found to be nonviable, both of the reversions identified in the genomes of L-rev1 and L-rev3 restored viral RNA synthesis, albeit not to the wild-type level. These results clearly demonstrated that second-site mutations in SL4 can indeed compensate for mutations introduced in SL5 and supported the existence and importance of the potential RNA pseudoknot structure formed by these two elements.

**The SL4-SL5 pseudoknot interaction is essential for EAV RNA synthesis.** To investigate the relevance of the proposed SL4-SL5 pseudoknot interaction in more detail, a series of mutants was generated in which the interaction was disrupted and subsequently restored without affecting the predicted structure of the individual hairpins (Fig. 5). In mutants Or4 and Or5, the orientations of the central pentanucleotide sequences in the SL4 and SL5 loops, respectively, were inverted to disrupt their interaction. Double mutant Or45 contained a combination of these mutations which should lead to a restoration of the base-pairing possibilities. In a second set of mutants, the central pentanucleotide sequences of the SL4 and SL5 loops were switched (mutants Sw4 and Sw5), again with restoration of base pairing predicted for double mutant Sw45.

BHK-21 cells were again transfected with the full-length RNA transcribed from wild-type and mutant EAV cDNA

A

| | SL5: 3'-5'<br>SL4: 5'-3' | IFA 14h | IFA 24h | IFA 40h | Titer* 24 hr |
|---|---|---|---|---|---|
| wt | UAUUGAUGAAGUUGUACUGC<br>GUUGCGCCUCCAGCAGGGCC | ++ | +++ | X | $8x10^6$ |
| loop2 | U*C*UU*C*AU*C*AAGUUGUACUGC<br>GUUGCGCCUCCAGCAGGGCC | - | - | - | $<10^3$ |
| L-rev1 | U*C*UU*C*AU*C*A**G**GUUGUACUGC<br>GUUGCGCCUCCAGCAGGGCC | + | ++ | +++ | $1x10^4$ |
| L-rev2 | U*C*UU*C*AU*C*A**G**GUUGUACUGC<br>GUUGCG**C**CUCCAGCAGGGCC | - | - | - | $<10^3$ |
| L-rev3 | U*C*UU*C*AU*C*AAGUUGUACUGC<br>GUUGCGCCU**U**CAGCAGGGCC | ++ | +++ | X | $3x10^5$ |

* titer in PFU/ml
X: cells detached and dying from infection

B

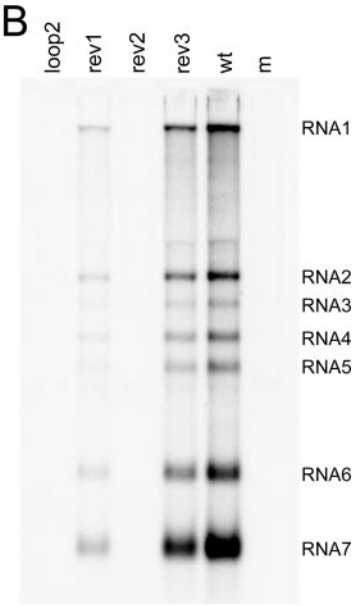


FIG. 4. Reversion of mutant Loop2. (A) Sequences of the 3′ terminal region of the genome of the Loop2 revertant were determined by RT-PCR, followed by sequencing of nine individual clones. Of the sequenced clones, seven were found to contain a second-site mutation in the SL5 loop region (L-rev1), but two clones acquired mutations in the SL4 domain. The revertant sequences were introduced into the wild-type EAV cDNA clone. Virus replication was studied using IFA with EAV-specific antisera for nsp3 and N at different time points after transfection, and virus titration was performed using plaque assays. The sequence of the SL5 loop region is depicted in the 3′-to-5′ direction, whereas that of SL4 is depicted in the 5′-to-3′ direction. Base-pairing possibilities between the two sequences are indicated by dots. The mutations introduced in the Loop2 mutant are marked in italics; the acquired reversions are marked by a black box. (B) Hybridization analysis of the RNA synthesis of the loop2 revertants (see the legend to Fig. 2 for details).

clones, and virus replication was monitored as described above. No IFA signal or infectivity was detected for the single mutants Or4 and Or5, whereas replication was restored in the double mutant Or45 (Table 3). Upon analysis of intracellular viral RNA synthesis (Fig. 6), there was no signal for the single mutants, whereas the RNA levels produced by double mutant Or45 approached those of the wild-type control. Also, for the Sw4 and Sw5 single mutants, RNA synthesis was completely disrupted (Fig. 6 and Table 3). Restoration of the base-pairing possibilities in double mutant Sw45 resulted in a low level of virus activity, as evidenced by the production of small quantities of intracellular viral RNA (Fig. 6) and a modestly positive IFA result (Table 3). However, for this double mutant, infectious progeny could not be detected in plaque assays, either because there was no virus production or, more likely, because the slow replication and low titers of this mutant virus were insufficient to allow plaque formation (as observed for other studies of severely crippled EAV mutants). Nevertheless, the results listed above, in particular those obtained with the Or4, Or5, and Or45 set of mutants, confirmed the critical importance for EAV RNA synthesis of both SL4 and SL5 loop sequences and their pseudoknot-type interaction.

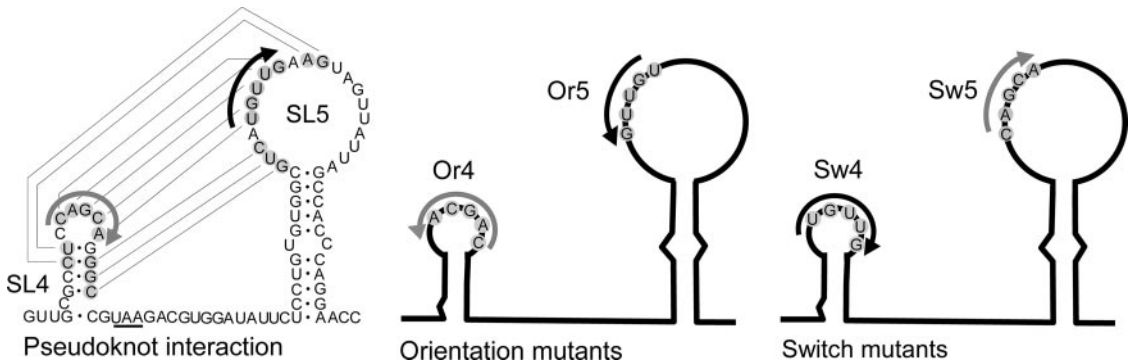


FIG. 5. RNA secondary structure model showing the proposed SL4-SL5 pseudoknot interaction and pseudoknot mutants. The nucleotides involved in the pseudoknot interaction are marked in gray, and the base-pairing interaction is depicted by lines. The orientation of the central pentanucleotide in the loop was changed in SL4 (Or4) or SL5 (Or5) or both (Or45), which restored base-pairing possibilities. The pentanucleotide sequence of SL4 was switched with that of SL5 in mutant Sw4, and vice versa in mutant Sw5. Base-pairing possibilities were again restored in mutant Sw45. The stop codon of the N protein gene is underlined.

TABLE 3. Viability of SL4-SL5 pseudoknot mutants

| Mutant | IFA at the indicated time points posttransfection | | | Titer (PFU/ml) at 24 h posttransfection |
|---|---|---|---|---|
| | 14 h | 24 h | 40 h | |
| wt | ++ | +++ | X | $7 \times 10^6$ |
| Or5 | − | − | − | ND |
| Or4 | − | − | − | ND |
| Or45 | ++ | +++ | X | $3 \times 10^6$ |
| Sw5 | − | − | − | ND |
| Sw4 | − | − | − | ND |
| Sw45 | + | ++ | +++ | $<10^3$ |

[a] X, cells were detached and dying from infection. ND, not determined.

**The SL4-SL5 pseudoknot interaction is conserved in evolution.** The natural sequence variation in the EAV SL4 and SL5 domains was analyzed to obtain phylogenetic support for the proposed pseudoknot interaction. However, the majority of sequences in a collection of EAV isolates was found to be identical to that of the Bucyrus isolate used in this study (Fig. 7). Only the Vienna isolate was found to contain a nucleotide change that creates an additional base pair, whereas the CW01 isolate was found to contain two nucleotide changes, both of which create an additional base pair in the interaction. Despite the limited variation observed, these nucleotide variations all supported the proposed pseudoknot interaction.

In addition, we tried to align the sequence of the 3′ end of the EAV genome with the corresponding domain of the other known arteriviruses, PRRSV (of European [EU] and North American [NA] genotypes), SHFV, and LDV, but obvious sequence conservation was not detected (results not shown). Subsequently, the RNA secondary structure of the 3′ proximal region of the different genomes was predicted using Mfold software. It was found that similar pairs of 3′ proximal hairpins can be predicted for all other arterivirus genomes (Fig. 8). Strikingly, in all cases, the potential for pseudoknot formation between the top region of the 3′ terminal hairpin (SL5 in EAV) and the upstream hairpin (SL4) was found, although the number of base pairs involved in this interaction differed.

To obtain further phylogenetic support for the proposed pseudoknot interactions, sequences from different isolates were aligned (Fig. 7). For PRRSV-NA, 27 other database entries were identical to that of standard isolate VR-2332. Covariation was observed for isolates Ingelvac, HB-1, and HB-2, in which a U-A base pair in the interaction was replaced by a C-G base pair. In a Taiwanese isolate, an additional base pair is created at the position of a mismatch in the proposed duplex. A nucleotide change creating a mismatch was found in four different PRRSV-NA isolates, in addition to several "neutral" nucleotide variations that do not affect base pairing. For PRRSV-EU, four other sequences were found to be identical to that of the standard Lelystad isolate. Strain EuroPRRSV was found to contain one neutral nucleotide change, and the Olot/91 isolate was found to contain two neutral changes and one change creating a mismatch. For LDV, all six of the other available sequences were identical to those of the LDV-P isolate. Taken together, the results of this comparative analysis suggested that the proposed SL4-SL5 pseudoknot interaction near the 3′ end of the EAV genome is a conserved feature in arterivirus evolution.

## DISCUSSION

Many important functions are associated with the 3′ terminus of RNA virus genomes, which may include initiation and regulation of minus-strand RNA synthesis, regulation of translation, participation in encapsidation, virion assembly, and possibly stabilization of the RNA molecule. In this study we have analyzed the RNA signals near the 3′ end of the genomic RNA of the EAV. The SL5 hairpin, located within the 3′ UTR just upstream of the poly(A) tail, was previously implicated in EAV RNA synthesis, presumably at the level of initiation of minus-strand RNA synthesis (3). Site-directed mutagenesis and reverse genetics were employed to define the essential components of this structural element. We demonstrated (Fig. 2) that it is the structure and not the sequence of the SL5 stem region that is important for viral RNA synthesis and that in particular, the large single-strand loop conformation and sequence of the SL5 loop are crucial (Fig. 1 to Fig. 3). Mfold predicted an alternative structure for the SL5 hairpin, with similar stability and part of the loop sequence engaged in internal base pairing. However, a mutation (mutant Open) that should prevent formation of this alternative structure had no significant effect (Fig. 2), suggesting that this fold is not required for EAV RNA synthesis. In addition, stabilization of the alternative fold (mutant Stable) was found to inhibit RNA synthesis and yielded a revertant in which both the sequence and the predicted fold of the large single-stranded SL5 loop had been restored (Fig. 3). Furthermore, several point mutations in the SL5 loop severely or completely inhibited RNA synthesis (Fig. 2).

Revertants obtained after prolonged culturing of the mutant Loop2 had acquired second-site mutations in either the SL5 loop (L-rev1) or the SL4 hairpin (Fig. 4A), suggesting a functional interaction between the SL5 and SL4 domains. The role of the acquired mutations in the phenotypic reversion of the loop2 mutant was verified by introduction of the revertant sequences into the wild-type EAV cDNA clone. The revertants L-rev1 and L-rev3 indeed gained replication capacity, but the

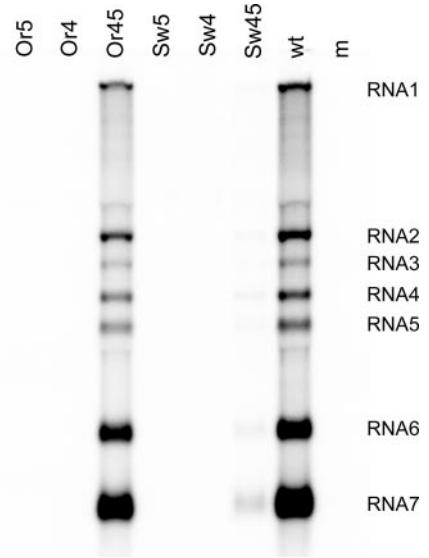


FIG. 6. Hybridization analysis of the RNA synthesis by wild-type EAV and pseudoknot mutants (see the legend to Fig. 2 for details).

| Virus | SL4-loop | SL5-loop | Accession number |
|---|---|---|---|
| **EAV** | | | |
| Bucyrus | cuccagcaggge | gucauguugaag | NC002532 |
| 15 others | ..... | ..... | |
| Vienna | ..u..... | ..... | X78497 |
| CW01 | ..u..... | ...c..... | AY349168 |
| **PRRSV-NA** | | | |
| VR2332 | cugauugacauugugccucua | ugggggugagauuuaauugg | U87392 |
| 27 others | ..... | ..... | |
| PL97-1 | ..... | .....u..... | AY585241 |
| CH-1a | .....c..... | ..... | AY032626 |
| HN1 | ..... | .....c..... | AY457635 |
| Prime pac | .....u..... | .....a..... | DQ779791 |
| IAF-exp91 | .....u..... | .....a.c..... | U02095 |
| P129 | ..... | .....a.a..... | AF494042 |
| Ingelvac | .....g..c..... | .....u.ag..... | DQ988080 |
| HB-2(sh)/2002 | .....c..... | .....a.ag..... | AY262352 |
| Japan | .....u..... | .....ag..... | D45852 |
| LMY | .....uc. | .....ca..... | DQ473474 |
| HB-1(sh)/2002 | .....c.....u.. | .....a.ag..... | AY150312 |
| Taiwan | .....ug..... | .....aua..... | AF121131 |
| **PRRSV-EU** | | | |
| Lelystad | gauuggcguguggccucug | ugggggucauacuuaauc | M96262 |
| 4 others | ..... | ..... | |
| EuroPRRSV | .....a..... | ..... | AY366525 |
| Olot/91 | .....a.....a | .....a..... | X92942 |
| **LDV** | | | |
| LDV-P | aguuacaa | uuguaauu | U15146 |
| 6 others | ..... | ..... | |

FIG. 7. Alignment of the nucleotides involved in the pseudoknot interaction in different arteriviruses. Several nucleotide changes were identified, as follows: those not disrupting base pairing (unmarked) and disrupting base pairing (black), those creating an additional base pair (dark gray), and covariations (light gray).

revertant L-rev2 appeared to be replication deficient (Fig. 4). The SL4 hairpin is located in the N protein gene, and the acquired mutations in both L-rev2 and L-rev3 affected the amino acid sequence of the N protein. The mutation found in L-rev3 was also identified in natural EAV isolates, indicating that it is unlikely to affect N protein function. On the other hand, in contrast to what has been suggested for coronaviruses (1, 2, 25, 37, 41), the arterivirus N protein was previously found to be dispensable for both replication and transcription (24, 31), since the L-rev2 sequence was cloned from RT-PCR on total cellular RNA, it could represent a nonreplicating genome.

The existence and importance of an SL4-SL5 base-pairing interaction was supported in more detail by using a series of mutants in which base pairing was disrupted and restored without affecting the structure of the individual hairpins (Fig. 6). These mutations only targeted the central pentanucleotide sequence located in the loop region, and the results would be consistent with an SL5-SL4 interaction consisting of a kissing loop interaction (i.e., involving only the unpaired nucleotides in the loop regions). However, the potential for a more extended SL4-SL5 pseudoknot interaction was discovered to consist of up to 10 base pairs (interrupted by two mismatches). Phylogenetic analysis revealed that the possibility for this extended SL4-SL5 interaction is conserved in different EAV isolates (Fig. 7). The mismatches were absent in two different isolates of EAV, and one mismatch was repaired in two different Loop2 revertants (Fig. 4). In addition, similar pseudoknot interactions can be predicted for the 3′-proximal domain of the genomes of all other arteriviruses (Fig. 8), which are only quite distantly related to EAV (11). Possibly due to this evolutionary distance, the predicted number of base pairs involved in the pseudoknot interaction is quite variable, and some mismatches appear to be permitted (Fig. 7). On the basis of these combined observations, we consider it likely that the SL5 and SL4 hairpins can indeed engage in the more extended pseudoknot interaction. A pair of 3′ proximal hairpins involved in a pseudoknot interaction may thus be a conserved feature of arterivirus genomes and one that, given its position in the genome and our results, is likely involved in regulating a critical step in viral of RNA synthesis.

A property inherent in RNA pseudoknots (32) is their low stability, which often results in the folding of alternative structures (8, 17, 34, 48). This feature enables them to function as "molecular switches," a situation also encountered, for example, elsewhere in the genome of EAV and all other nidoviruses, where an RNA pseudoknot is a key element of the ribosomal frameshift-inducing mechanism that regulates expression of replicase ORF1b (4, 5). The SL4-SL5 pseudoknot interaction now identified in the 3′ proximal domain of the EAV genome is essential for viral RNA synthesis, most likely by playing a role in the initiation of minus-strand RNA synthesis. Possibly, the pseudoknot conformation is specifically recognized by the viral replicase complex, and switching to or from a conformation containing the individual SL4 and SL5 hairpins could regulate the specificity or timing of an apparently critical step in arterivirus RNA synthesis.

The genomes of plus-strand RNA viruses are not only templates for RNA synthesis, but are also directly translated to

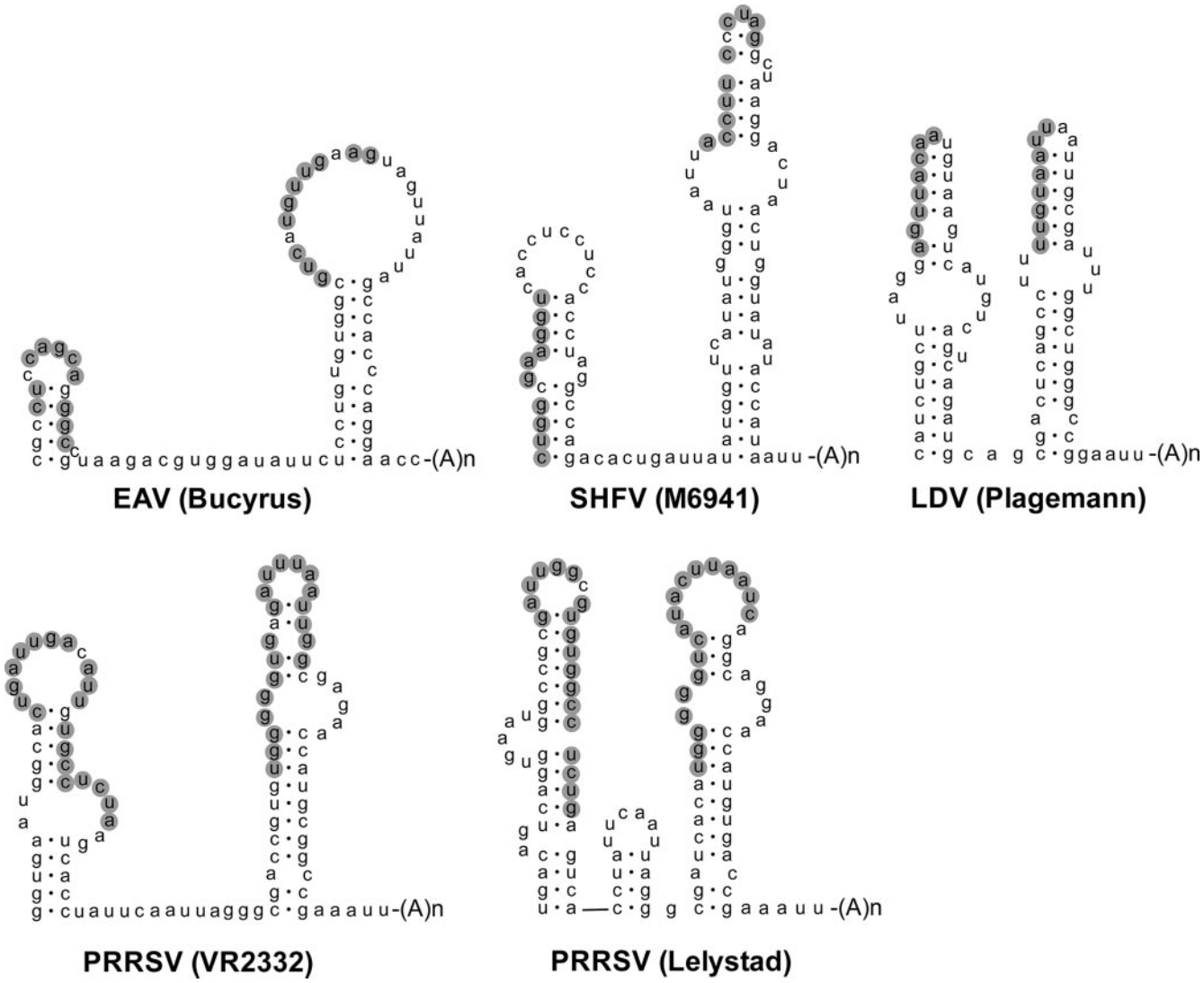


FIG. 8. Conservation of the pseudoknot interaction in all known arteriviruses. The RNA secondary structure predictions for the two terminal stem-loop structures in different arterivirus genomes are shown. For all arteriviruses, a putative interaction between the top region of the terminal hairpin and the upstream hairpin is predicted and is marked in gray. Shown are EAV (Brucyrus [accession number NC002532]), SHFV (M6941 [accession number NC003092]), LDV (Plagemann [accession number U15146]), PRRSV (VR2332 [accession number U87392]), and PRRSV (Lelystad [accession number M96262]).

yield viral proteins. Opposing the model in which every genomic RNA molecule is used for both translation and RNA synthesis stands a model in which RNA molecules may have a designated function, at least later in infection. Replication of the genome of EAV and other plus-strand RNA viruses takes place in complexes that are associated with cytoplasmic membranes and contain both viral and host proteins. It has been speculated that this compartmentalization may serve to create an optimal environment for RNA synthesis (7, 21, 40). According to this model, the local concentration of essential factors in a given compartment could determine whether translation or replication would be favored, maintaining two separate pools of genomic RNAs. Studies of RNA synthesis suggested that this is not the case for poliovirus. Viral RNA replication was found to depend on translation in *cis* of the genome, suggesting that a particular viral genome must first be translated to become competent for RNA synthesis (26). These results imply that for poliovirus and possibly other plus-strand RNA viruses, each viral RNA genome has a dual role which would require regulation throughout the entire virus life cycle. Viral RNA synthesis in poliovirus and other enteroviruses was suggested to be regulated by a pseudoknot interaction in the 3′ UTR (15, 22). Pseudoknots are present near the 3′ end of many viral RNA genomes and may be optimally suited to function as a molecular switch regulating the initiation of RNA synthesis.

For PRRSV, an additional kissing loop interaction between the upstream stem-loop involved in the proposed pseudoknot (the "equivalent" of EAV SL4) and a hairpin located in the N protein gene was previously suggested to be required for virus replication (46). The pseudoknot and the kissing loop interaction are mutually exclusive interactions, which may both act as molecular switches in different stages of the PRRSV life cycle.

However, a similar kissing loop interaction could not be predicted in the genomes of EAV and other arteriviruses. Coronaviruses have a longer and more complex 3′ UTR than arteriviruses, and we were unable to identify a pseudoknot interaction similar to that in EAV, involving a 3′ terminal hairpin. However, a conserved pseudoknot in sequences more upstream in the coronavirus 3′ UTR has been documented (9, 9, 12, 13, 47). This pseudoknot interaction was also proposed to act as a molecular switch during virus replication, but it is currently unknown whether it could be the functional equivalent of the one described here for arteriviruses. Although none of them mapped to the region containing the pseudoknot, several protein binding sites were reported in the coronavirus 3′ UTR. For example, four cellular proteins were found to bind the 3′ terminus of the mouse hepatitis virus (MHV) genome (49, 50), and a binding site for the hnRNP A1 was mapped to the 3′ proximal region of the MHV genome (14). However, these binding sites could be deleted without a significant effect on viral replication or RNA synthesis (10).

Depending on the energy barrier between the conformation with individual SL4 and SL5 hairpins and the pseudoknot conformation in the EAV 3′ genome terminus, the putative switch could be self-induced or require *trans*-acting elements. Previously, pseudoknot formation was not detected during in vitro chemical and enzymatic probing experiments (3). This suggests that in vivo *trans*-acting factors may be involved in pseudoknot formation. Alternatively, the pseudoknot may be a very unstable and transient interaction that cannot be detected using biochemical probing. A recent study of SHFV described binding of two cellular proteins to the stem-loop structure at the 3′ end of the genome, which were identified as polypyrimidine tract-binding protein and aldolase A (18, 19). The same proteins were reported to interact with the 3′ UTR of the EAV and PRRSV genomes (19), but the biological role and importance of these interactions with the 3′ UTR remain to be investigated. Our ongoing studies will focus on identification of cellular and viral proteins that bind specifically to the hairpin or pseudoknot structures in the EAV genome, and could be involved in a putative switch between these conformations.

## ACKNOWLEDGMENTS

We thank Sjoerd van den Worm, Erwin van den Born, and Willy Spaan for helpful discussions.

Nancy Beerens was supported by Veni grant 700.53.405 from the Council for Chemical Sciences of The Netherlands Organization for Scientific Research (NWO-CW).

## REFERENCES

1. **Almazan, F., C. Galan, and L. Enjuanes.** 2004. The nucleoprotein is required for efficient coronavirus genome replication. J. Virol. **78:**12683–12688.
2. **Baric, R. S., G. W. Nelson, J. O. Fleming, R. J. Deans, J. G. Keck, N. Casteel, and S. A. Stohlman.** 1988. Interactions between coronavirus nucleocapsid protein and viral RNAs: implications for viral transcription. J. Virol. **62:**4280–4287.
3. **Beerens, N., and E. J. Snijder.** 2006. RNA signals in the 3′ terminus of the genome of equine arteritis virus are required for viral RNA synthesis. J. Gen. Virol. **87:**1977–1983.
4. **Brierley, I., P. Digard, and S. C. Inglis.** 1989. Characterization of an efficient coronavirus ribosomal frameshifting signal: requirement for an RNA pseudoknot. Cell **57:**537–547.
5. **den Boon, J. A., E. J. Snijder, E. D. Chirnside, A. A. de Vries, M. C. Horzinek, and W. J. M. Spaan.** 1991. Equine arteritis virus is not a togavirus but belongs to the coronaviruslike superfamily. J. Virol. **65:**2910–2920.
6. **DeRijk, P., and R. DeWachter.** 1997. RnaViz, a program for the visualisation of RNA secondary structure. Nucleic Acids Res. **25:**4679–4684.
7. **Enjuanes, L., F. Almazan, I. Sola, and S. Zuniga.** 2006. Biochemical aspects of coronavirus replication and virus-host interaction. Annu. Rev. Microbiol. **60:**211–230.
8. **Gluick, T. C., R. B. Gerstner, and D. E. Draper.** 1997. Effects of Mg2+, K+, and H+ on an equilibrium between alternative conformations of an RNA pseudoknot. J. Mol. Biol. **270:**451–463.
9. **Goebel, S. J., B. Hsue, T. F. Dombrowski, and P. S. Masters.** 2004. Characterization of the RNA components of a putative molecular switch in the 3′ untranslated region of the murine coronavirus genome. J. Virol. **78:**669–682.
10. **Goebel, S. J., T. B. Miller, C. J. Bennett, K. A. Bernard, and P. S. Masters.** 2007. A hypervariable region within the 3′ *cis*-acting element of the murine coronavirus genome is nonessential for RNA synthesis but affects pathogenesis. J. Virol. **81:**1274–1287.
11. **Gorbalenya, A. E., L. Enjuanes, J. Ziebuhr, and E. J. Snijder.** 2006. Nidovirales: evolving the largest RNA virus genome. Virus Res. **117:**17–37.
12. **Hsue, B., T. Hartshorne, and P. S. Masters.** 2000. Characterization of an essential RNA secondary structure in the 3′ untranslated region of the murine coronavirus genome. J. Virol. **74:**6911–6921.
13. **Hsue, B., and P. S. Masters.** 1997. A bulged stem-loop structure in the 3′ untranslated region of the genome of the coronavirus mouse hepatitis virus is essential for replication. J. Virol. **71:**7567–7578.
14. **Huang, P., and M. M. Lai.** 2001. Heterogeneous nuclear ribonucleoprotein A1 binds to the 3′-untranslated region and mediates potential 5′-3′-end cross talks of mouse hepatitis virus RNA. J. Virol. **75:**5009–5017.
15. **Jacobson, S. J., D. A. M. Konings, and P. Sarnow.** 1993. Biochemical and genetic-evidence for a pseudoknot structure at the 3′ terminus of the poliovirus RNA genome and its role in viral RNA amplification. J. Virol. **67:**2961–2971.
16. **Koev, G., S. J. Liu, R. Beckett, and W. A. Miller.** 2002. The 3′-terminal structure required for replication of barley yellow dwarf virus RNA contains an embedded 3′ end. Virology **292:**114–126.
17. **Kolk, M. H., M. van der Graaf, S. S. Wijmenga, C. W. A. Pleij, H. A. Heus, and C. W. Hilbers.** 1998. NMR structure of a classical pseudoknot: interplay of single- and double-stranded RNA. Science **280:**434–438.
18. **Maines, T. R., and M. A. Brinton.** 2001. Identification of cell proteins that bind to the SHFV 3′ (+)NCR. Adv. Exp. Med. Biol. **494:**647–653.
19. **Maines, T. R., M. Young, N. N. Dinh, and M. A. Brinton.** 2005. Two cellular proteins that interact with a stem loop in the simian hemorrhagic fever virus 3′(+)NCR RNA. Virus Res. **109:**109–124.
20. **Mandal, M., and R. R. Breaker.** 2004. Gene regulation by riboswitches. Nat. Rev. Mol. Cell. Biol. **5:**451–463.
21. **Masters, P. S.** 2006. The molecular biology of coronaviruses, p. 193–292. *In* K. Maramorosch and A. Shatkin (ed.), Advances in virus research, 66. Academic Press, New York, NY.
22. **Mirmomeni, M. H., P. J. Hughes, and G. Stanway.** 1997. An RNA tertiary structure in the 3′ untranslated region of enteroviruses is necessary for efficient replication. J. Virol. **71:**2363–2370.
23. **Molenkamp, R., S. Greve, W. J. M. Spaan, and E. J. Snijder.** 2000. Efficient homologous RNA recombination and requirement for an open reading frame during replication of equine arteritis virus defective interfering RNAs. J. Virol. **74:**9062–9070.
24. **Molenkamp, R., H. van Tol, B. C. Rozier, Y. van der Meer, W. J. M. Spaan, and E. J. Snijder.** 2000. The arterivirus replicase is the only viral protein required for genome replication and subgenomic mRNA transcription. J. Gen. Virol. **81:**2491–2496.
25. **Nelson, G. W., S. A. Stohlman, and S. M. Tahara.** 2000. High affinity interaction between nucleocapsid protein and leader/intergenic sequence of mouse hepatitis virus RNA. J. Gen. Virol. **81:**181–188.
26. **Novak, J. E., and K. Kirkegaard.** 1994. Coupling between genome translation and replication in an RNA virus. Genes Dev. **8:**1726–1737.
27. **Nudler, E., and A. S. Mironov.** 2004. The riboswitch control of bacterial metabolism. Trends Biochem. Sci. **29:**11–17.
28. **Olsthoorn, R. C., S. Mertens, F. T. Brederode, and J. F. Bol.** 1999. A conformational switch at the 3′ end of a plant virus RNA regulates viral replication. EMBO J. **18:**4856–4864.
29. **Pasternak, A. O., A. P. Gultyaev, W. J. M. Spaan, and E. J. Snijder.** 2000. Genetic manipulation of arterivirus alternative mRNA leader-body junction sites reveals tight regulation of structural protein expression. J. Virol. **74:**11642–11653.
30. **Pasternak, A. O., W. J. M. Spaan, and E. J. Snijder.** 2006. Nidovirus transcription: how to make sense. J. Gen. Virol. **87:**1403–1421.
31. **Pasternak, A. O., E. van den Born, W. J. M. Spaan, and E. J. Snijder.** 2001. Sequence requirements for RNA strand transfer during nidovirus discontinuous subgenomic RNA synthesis. EMBO J. **20:**7220–7228.
32. **Pleij, C. W. A.** 1994. RNA pseudoknots. Curr. Opin. Struct. Biol. **4:**337–344.
33. **Pogany, J., M. R. Fabian, K. A. White, and P. D. Nagy.** 2003. A replication silencer element in a plus-strand RNA virus. EMBO J. **22:**5602–5611.
34. **Puglisi, J. D., J. R. Wyatt, and I. Tinoco.** 1990. Conformation of an RNA pseudoknot. J. Mol. Biol. **214:**437–453.
35. **Sawicki, S. G., and D. L. Sawicki.** 1995. Coronaviruses use discontinuous extension for synthesis of subgenome-length negative strands. Adv. Exp. Med. Biol. **380:**499–506.

36. **Sawicki, S. G., D. L. Sawicki, and S. G. Siddell.** 2007. A contemporary view of coronavirus transcription. J. Virol. **81:**20–29.
37. **Schelle, B., N. Karl, B. Ludewig, S. G. Siddell, and V. Thiel.** 2005. Selective replication of coronavirus genomes that express nucleocapsid protein. J. Virol. **79:**6620–6630.
38. **Schuppli, D., J. Georgijevic, and H. Weber.** 2000. Synergism of mutations in bacteriophage Q. beta RNA affecting host factor dependence of Q. beta replicase. J. Mol. Biol. **295:**149–154.
39. **Snijder, E. J., S. G. Siddell, and A. E. Gorbalenya.** 2005. The order Nidovirales, p. 390–404. *In* B. W. Mahy and V. ter Meulen (ed.), Topley and Wilson's microbiology and microbial infections. Hodder Arnold, London, United Kingdom.
40. **Snijder, E. J., Y. van der Meer, J. Zevenhoven-Dobbe, J. J. M. Onderwater, J. van der Meulen, H. K. Koerten, and A. M. Mommaas.** 2006. Ultrastructure and origin of membrane vesicles associated with the severe acute respiratory syndrome coronavirus replication complex. J. Virol. **80:**5927–5940.
41. **Stohlman, S. A., R. S. Baric, G. N. Nelson, L. H. Soe, L. M. Welter, and R. J. Deans.** 1988. Specific interaction between coronavirus leader RNA and nucleocapsid protein. J. Virol. **62:**4288–4295.
42. **Sudarsan, N., J. E. Barrick, and R. R. Breaker.** 2003. Metabolite-binding RNA domains are present in the genes of eukaryotes. RNA **9:**644–647.
43. **van den Born, E., C. C. Posthuma, A. P. Gultyaev, and E. J. Snijder.** 2005. Discontinuous subgenomic RNA synthesis in arteriviruses is guided by an RNA hairpin structure located in the genomic leader region. J. Virol. **79:**6312–6324.
44. **van der Meer, Y., H. van Tol, J. Krijnse Locker, and E. J. Snijder.** 1998. ORF1a-encoded replicase subunits are involved in the membrane association of the arterivirus replication complex. J. Virol. **72:**6689–6698.
45. **van Dinten, L. C., J. A. den Boon, A. L. M. Wassenaar, W. J. M. Spaan, and E. J. Snijder.** 1997. An infectious arterivirus cDNA clone: identification of a replicase point mutation that abolishes discontinuous mRNA transcription. Proc. Natl. Acad. Sci. USA **94:**991–996.
46. **Verheije, M. H., R. C. L. Olsthoorn, M. V. Kroese, P. J. M. Rottier, and J. J. M. Meulenberg.** 2002. Kissing interaction between 3′ noncoding and coding sequences is essential for porcine arterivirus RNA replication. J. Virol. **76:**1521–1526.
47. **Williams, G. D., R. Y. Chang, and D. A. Brian.** 1999. A phylogenetically conserved hairpin-type 3′ untranslated region pseudoknot functions in coronavirus RNA replication. J. Virol. **73:**8349–8355.
48. **Wyatt, J. R., J. D. Puglisi, and I. J. Tinoco.** 1990. RNA pseudoknots: sStability and loop size requirements. J. Mol. Biol. **214:**455–470.
49. **Yu, W., and J. L. Leibowitz.** 1995. A conserved motif at the 3′ end of mouse hepatitis virus genomic RNA required for host protein binding and viral RNA replication. Virology **214:**128–138.
50. **Yu, W., and J. L. Leibowitz.** 1995. Specific binding of host cellular proteins to multiple sites within the 3′ end of mouse hepatitis virus genomic RNA. J. Virol. **69:**2016–2023.
51. **Zhang, G. H., J. C. Zhang, and A. E. Simon.** 2004. Repression and derepression of minus-strand synthesis in a plus-strand RNA virus replicon. J. Virol. **78:**7619–7633.
52. **Zuker, M.** 1989. On finding all suboptimal foldings of an RNA molecule. Science **244:**48–52.
53. **Zuker, M.** 2003. Mfold web server for nucleic acid folding and hybridization prediction. Nucleic Acids Res. **31:**3406–3415.